J Therm Anal Calorim (2011) 105:83–91
DOI 10.1007/s10973-011-1524-7

Structure and evolved gas analyses (TG/DTA-MS and TG-FTIR) of *mer*-trichlorotris(thiourea)-indium(III), a precursor for indium sulfide thin films

Kairi Otto · Petra Bombicz · János Madarász · Ilona Oja Acik · Malle Krunks · György Pokol

Niinistö"s Special Chapter

Abstract The indium complex, *mer*-trichlorotris(thiourea)-indium(III) ($In(tu)_3Cl_3$, **1**), crystallized from aqueous solution of $InCl_3$ and $SC(NH_2)_2$ (tu) with molar ratio of 1:3, is a single-source precursor for In_2S_3 films by chemical spray pyrolysis. The structural model of the triclinic crystal **1** (space group *P*-1 with $a = 8.4842(2)$ Å, $b = 10.5174(2)$ Å, $c = 13.1767(2)$ Å, $\alpha = 111.1870(10)°$, $\beta = 98.0870(10)°$, $\gamma = 97.889(2)°$) has been improved by single crystal X-ray diffraction analysis through successful separation of the disordered positions of the asymmetric complex molecule situated on the inversion centre into two spatial arrangements. Thermal decomposition of **1** occurs with very similar mass loss courses till 400 °C in both nitrogen and air, anyhow the DTA curve indicates a gas-phase oxidation with an additional exothermic heat effect at 255 °C in air. Partial or more advanced oxidation of the initially evolved CS_2 has taken place in both atmospheres, as its oxidation products, SO_2, COS, CO_2 are accompanied by the release of NH_3, HCl in temperature range of 205–275 °C, while H_2NCN and HCN evolve in air. In the third mass loss step, in the temperature interval of 405–750 °C in nitrogen and 405–700 °C in air, two processes, evaporation and oxidation of the solid residues are competing with each other, resulting in final decomposition product of **1** in air In_2O_3, while also some In_2O_3 in inert atmosphere beyond the main phase of In_2S_3 where, in addition considerable extent of loss of indium occurs, probably through volatile dimeric indium chloride species, which could not be detected either by EGA-MS or EGA-FTIR systems of ours. Nevertheless, evolution of HNCS is confirmed by EGA-FTIR, and release of CO_2, H_2NCN, SO_2, and a little HCl is detected at temperatures above 450 °C in both atmospheres.

Keywords Indium sulfide · Chemical spray pyrolysis · Thiourea · Indium chloride · Single crystal X-ray diffraction · Simultaneous thermogravimetry (TG) and differential thermal analysis (DTA) · Evolved gas analysis (EGA) · Mass spectrometry (MS) · FTIR spectroscopy

Introduction

Chemical spray pyrolysis (CSP) is a simple, fast and economical method to deposit thin films. The studies on the formation of various metal sulfide thin films (e.g., CdS, ZnS, Cu_xS) in the CSP process, including the formation of intermediates in the spray solution, their structure and thermal degradation, have been carried out over the past 16 years with more than 10 articles by an informal international research group leaded by Professor Lauri Niinistö. This work is a continuation of our previous studies whereby we expand the list of the metal sulfides with indium sulfide (In_2S_3).

K. Otto · I. Oja Acik · M. Krunks (✉)
Department of Materials Science, Tallinn University of Technology, Ehitajate tee 5, Tallinn 19086, Estonia
e-mail: malle@staff.ttu.ee

P. Bombicz
Institute of Structural Chemistry, Chemical Research Center, Hungarian Academy of Sciences, POB 17, Budapest 1525, Hungary

J. Madarász · G. Pokol
Department of Inorganic and Analytical Chemistry, Budapest University of Technology and Economics, Szt. Gellért tér 4, Budapest 1521, Hungary

In_2S_3 thin films deposited by the CSP method have been used as a buffer layer instead of CdS in chalcopyrite absorber based photovoltaic structures [1, 2]. Aqueous or alcoholic solutions containing indium chloride ($InCl_3$) and thiourea ($SC(NH_2)_2$) have been generally used for In_2S_3 thin films deposition by CSP. It has been found that the molar ratio of In and S sources (In:S) in the spray solution and the deposition temperature are the main parameters controlling the phase and chemical composition, structure, and optical properties of the sprayed In_2S_3 film [2–5].

Recently, we presented the thermal degradation of precursors for CSP–In_2S_3 films obtained by drying of aqueous spray solutions containing $InCl_3$ and $SC(NH_2)_2$ (tu) at molar ratios of 1:3 and 1:6 [6]. Thermal degradation of these two precursors was studied in air, with emphasis to solid decomposition products by ex situ XRD and FTIR [6]. Furthermore, the results indicated that the dried precursor from the solution with the In:S molar ratio of 1:3 was an indium chloride thiourea complex compound, while dried precursor from the solution with the In:S molar ratio of 1:6 contains an indium chloride thiourea complex compound and excess of crystalline $SC(NH_2)_2$.

Malyarik et al. [7] studied the crystal structure of $In(tu)_3Cl_3$ obtained from an aqueous solution containing $InCl_3$ and $SC(NH_2)_2$ in molar ratio of 1:1 and 1:3. The $In(tu)_3Cl_3$ complex was triclinic, with space group *P*-1, $a = 8.519(2)$ Å, $b = 10.555(2)$ Å, $c = 13.325(2)$ Å, $\alpha = 111.30(2)°$, $\beta = 99.00(1)°$, $\gamma = 97.68(2)°$, $V = 1078.7(4)$ Å^3, $Z = 3$. However, the atomic structural resolution of a disordered asymmetric complex molecule situated on the inversion centre proved to be improper that time.

Therefore this study has two aims, firstly, to re-determine the structure of trichlorotris(thiourea)-indium(III) complex compound ($In(tu)_3Cl_3$) obtained from solution containing $InCl_3$ and $SC(NH_2)_2$ in molar ratio of 1:3, and secondly, to characterize its thermal behavior in an inert and oxidative atmospheres by simultaneous thermogravimetric and differential thermal analysis coupled online with quadrupole mass spectrometer (TG/DTA-MS) or FTIR spectrometric gas cell (TG-FTIR).

Experimental

Preparation of samples

Thiourea ($SC(NH_2)_2$) (p.a. > 98%, Merck S32896) and indium(III)chloride ($InCl_3$) aqueous solution were employed for the synthesis of the precursor for thermal analysis. For the preparation of $InCl_3$ solution, indium wire (p.a. 99.99%, Alfa Aesar) was dissolved in concentrated hot hydrochloric acid (Merck). The prepared 0.1 M $InCl_3$ aqueous solution had the pH value of 2.2.

The precursor solution was prepared by mixing the aqueous solutions of 0.1 M $InCl_3$ and 0.75 M $SC(NH_2)_2$ at room temperature. The $InCl_3$ and $SC(NH_2)_2$ molar ratio was 1:3, with the $[In^{3+}]$ concentration of 5×10^{-2} mol/L. The solution was let to evaporate slowly at 50 °C in a laboratory oven for a week. The obtained dried powder of $In(tu)_3Cl_3$ (**1**) (tu for thiourea) was used for thermal analysis.

Small single crystals of **1** were obtained on the vertical walls of an elongated cylindrical glass vessel from saturated solution of the powdered sample in 0.5 mL of distilled water during recrystallisation.

Elemental analysis

According to elemental analysis carried out at the Microanalytical Laboratory of Loránd Eötvös University of Budapest (ELTE-TTK, Budapest, Hungary) on a Vario ELIII (Elementaranalyse) CHN microanalyser system, the measured elemental composition of **1** (found, in mass%) was: S 21.23%, Cl 23.14%, N 18.05%, C 8.13%, H 2.88%. The elemental composition of **1** is close to that calculated for $In(tu)_3Cl_3$ (in mass%): S 21.40%, Cl 23.66%, N 18.69%, C 8.02%, H 2.69%. According to FTIR study, in **1** the thiourea is coordinated to the In cation via its S atom [6].

Structure determination and refinement

Crystal data: Molecular formula: $C_3H_{12}Cl_3InN_6S_3$, Fwt.: 449.55, triclinic crystal system, space group *P*-1, $a = 8.4842(2)$ Å, $b = 10.5174(2)$ Å, $c = 13.1767(2)$ Å, $\alpha = 111.1870(10)°$, $\beta = 98.0870(10)°$, $\gamma = 97.889(2)°$, $V = 1062.63(4)$ Å^3, $Z = 3$, $Z' = 1.5$, $F(000) = 220$, $Dx = 2.098$ Mg/m^3, $\mu = 22.570$ mm^{-1}.

A colorless, prism single crystal of $In(tu)_3Cl_3$ (**1**) having the size of $0.32 \times 0.18 \times 0.15$ mm was mounted on a loop. Cell parameters were determined by least-squares of the setting angles of 9296 ($6.90 \leq \theta \leq 61.42°$) reflections. Intensity data were collected on an RAXIS-RAPID diffractometer (graphite monochromator; Cu-Kα radiation, $\lambda = 1.54178$ Å) at 113(2) K in the θ range of $6.93 \leq \theta \leq 71.83°$, and *hkl* range of $-9 \leq h \leq 8$, $-12 \leq k \leq 12$, $-16 \leq l \leq 16$ using dtprofit.ref scans.

In all, 14919 reflections were collected of which 3309 were unique [$R(\text{int}) = 0.0888$, $R(\text{sigma}) = 0.0675$]; 3008 reflections were $>2\sigma(I)$. An empirical absorption correction was applied to the data (the minimum and maximum transmission factors were 0.0521 and 0.1328). The structure was solved by direct methods [8]. Anisotropic full-matrix least-squares refinement on F^2 [8] for all non-hydrogen atoms yielded $R_1 = 0.0724$ and $wR_2 = 0.1812$

for 3008 [$I > 2\sigma\ (I)$] and $R_1 = 0.0791$ and $wR_2 = 0.1948$ for all (3309) intensity data (goodness-of-fit = 1.069; the maximum and mean shift/esd 0.652 and 0.004). Number of parameters was 185. The weighting scheme applied was $w = 1/[\sigma^2(F_o^2) + (0.0965P)^2 + 23.5937P]$, where $P = (F_o^2 + 2F_c^2)/3$.

Hydrogen atomic positions were calculated from assumed geometries. Hydrogen atoms were included in the structure factor calculations but they were not refined. The isotropic displacement parameters of the hydrogen atoms were approximated from the U(eq) value of the atom they were bonded.

Crystallographic data (excluding structure factors) for the above crystal structure have been deposited with the Cambridge Crystallographic Data Centre as supplementary publication number CCDC 816601.

In situ EGA by coupled TG/DTA-MS

An STD 2960 Simultaneous TG/DTA apparatus (TA Instruments, USA), heating rate of 10 °C min^{-1}, purge gas (nitrogen or air) with a flow rate of 130 mL/min, sample sizes 8.71 mg (in nitrogen), and 9.60 mg (in air) in open Pt crucible was used. Mixture of gaseous species could reach a ThermoStar GDS 300 (Balzers Instruments) quadrupole mass spectrometer equipped with Chaneltron detector, through a heated 100% methyl deactivated fused silica capillary tubing kept at $T = 200$ °C. Data collection was carried out with QuadStar 422v60 software in multiple ion detection mode (MID) monitoring 64 channels ranging between $m/z = 1$–300. Measuring time was ca. 0.5 s for a channel.

In situ EGA by coupled TG-FTIR

A TGA 2050 Thermogravimetric Analyzer (TA Instruments, USA) with a heating rate of 10 °C min^{-1}, with air flow rate of 120 mL/min (and an extra 10 mL/min air as a balance purge) and sample size 8.69 mg in open Pt crucible was used. Gaseous species evolved from **1** were led to FTIR gas cell of a BioRad TGA/IR Accessory Unit equipped with cooled DTGS detector through a heated stainless steel transfer line ($l = 90$ cm, $d = 4$ mm) kept at $T = 200$ °C. FTIR spectra (600–4000 cm^{-1}) were collected in every 30 s after accumulation of 29 interferograms by a BioRad Excalibur Series FTS 3000 spectrometer using Win IR Pro 2.7 FTIR (BioRad) data collection and evaluation software.

The evolved gases were identified on the basis of their MS and FTIR reference spectra available in the public domain spectral libraries of NIST [9] and literature [17].

Results and discussion

Crystal structure of $In(tu)_3Cl_3$ (**1**)

Figure 1 shows the ORTEP representation [10] of the two crystallographically independent complex molecules both in *mer*-configuration in the crystal structure of $In(tu)_3Cl_3$ (**1**), i.e., *mer*- or (OC-6-21)-trichlorotris(thiourea)-indium(III). There is 1.5 indium complex molecules in the asymmetric unit. One of the molecules is in general position. The In core of the other molecule is in special position laying in the origo. Thus, half of the molecule belongs to the asymmetric unit, the other half is symmetry generated by the inversion centre. As a consequence of the odd number of ligands, this molecule is disordered. The found atomic positions can be separated into two different conformations of the complex (Fig. 2). Although the structure of $In(tu)_3Cl_3$ (**1**) was reported [7] in 1992, the disordered separation of the two complex forms present in the crystal structure has been published only now.

The thiourea and chloride ligands around the indium cation are placed in octahedral arrangement to be meridional isomers in all three crystallographic forms. The average In–Cl coordinative bond length is 2.535 Å, while the average In–S distance is 2.605 Å. The unit cell contains no residual solvent accessible void.

Thermal analysis

According to TG curves of **1** (Fig. 3), the thermal degradation in the temperature range of 205–800 °C in nitrogen and in air atmospheres consisted of three mass loss steps. All decomposition steps in nitrogen were endothermic processes, while in air also exothermic processes were observed (Fig. 4).

The first mass loss step in both atmospheres was in the temperature range of 205–275 °C with similar mass losses of ca. 33.9%. In nitrogen, four endothermic reactions occurred with maxima at 210, 215, 230, and 255 °C (Fig. 4). In air, the first mass loss step of **1** started with two endothermic reactions with maxima at 210, 215 °C, which immediately changed to an exothermic process peaked at 230 °C, followed by an endothermic reaction with a maximum at 255 °C (Fig. 4).

The second decomposition step in the temperature range of 275-405 °C was an endothermic process with DTA maximum at 320 °C in both atmospheres (Fig. 4). The mass losses in the second step were 13.2% in both atmospheres.

The third decomposition step started at 405 °C, and continued up to 750 °C in nitrogen and up to 700 °C in air (Fig. 3). In nitrogen, one endothermic reaction occurred with a maximum at 610 °C (Fig. 4). In air, the third mass

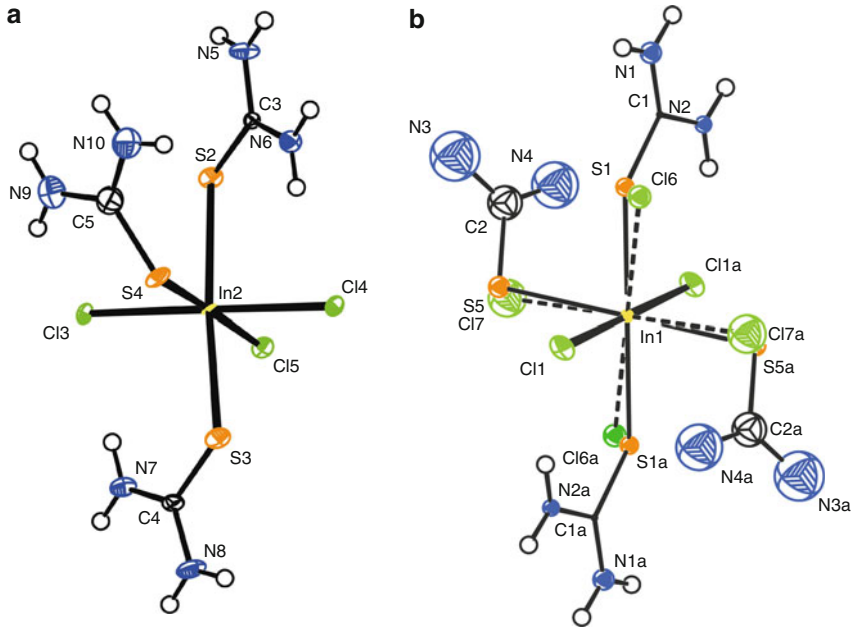

Fig. 1 ORTEP representation [10] of the two crystallographically independent molecules in the asymmetric unit of $In(tu)_3Cl_3$ (**1**) at 50% probability level. **a** The complex molecule in general position. **b** The disordered complex molecule organized by the symmetry centre

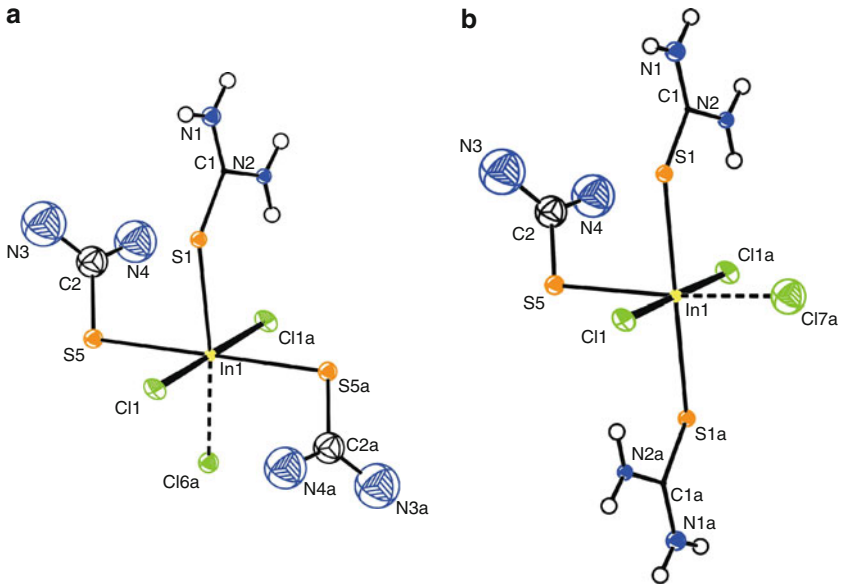

Fig. 2 The different conformations of the complex molecule of $In(tu)_3Cl_3$ (**1**) situated in the origo. The disordered positions can be separated into two different complex arrangements **a** and **b**, both having meridional arrangement

loss step (405–700 °C) was a two-step exothermic process with DTA maxima at 605 and 670 °C (Fig. 4). The mass losses in the third step were 29.1 and 25.7% in nitrogen and in air, respectively.

According to XRD, the final decomposition product of **1** at 800 °C in nitrogen consisted of In_2S_3 (JCPDS 01-074-7284) [11] and In_2O_3 (JCPDS 01-071-2194) [11] in amount of 92 and 8%, respectively. The final decomposition product of **1** at 800 °C in air was In_2O_3 (JCPDS 01-071-2194).

The total mass loss in the course of the thermal degradation of **1** was 76.1% in nitrogen and 72.8% in air. According to the phase composition of the final products, the total mass loss should be 64.2 and 69.1% in nitrogen and in air, respectively. Thus, the total mass loss of **1** in both atmospheres was higher than the calculated value indicating the release of some volatile indium species in both atmospheres and specially in nitrogen. This result is in agreement with that observed for the sample **1** in air using SetSys-Evolution thermal analysis instrument [6]. Higher mass loss than expected was also observed in the case of the thermal decomposition of the zinc chloride thiourea complex ($Zn(SCN_2H_4)_2Cl_2$) and was explained by the evaporation of $ZnCl_2$ [12, 13]. In current case likely volatile indium chloride, as an intermediate decomposition product, could be responsible for the loss of indium due to its relatively high vapor pressure at elevated temperatures [14].

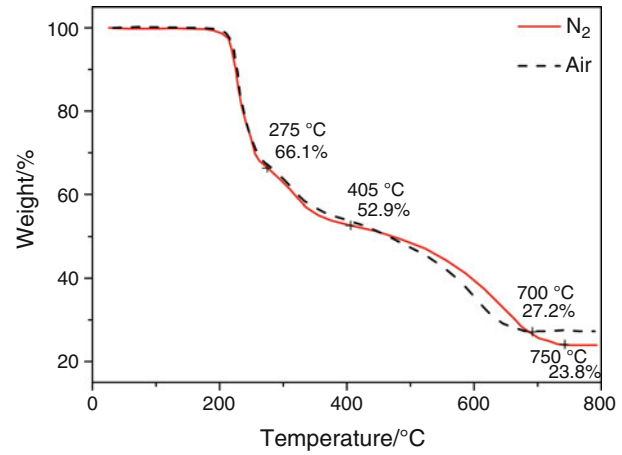

Fig. 3 TG curves of **1** in nitrogen (*solid line*) and air (*dashed line*), as measured in situ in the online coupled TG/DTA-MS system. N_2 flow 130 mL/min, heating rate 10 °C/min, initial mass 8.71 mg; air flow 130 mL/min, heating rate 10 °C/min, initial mass 9.60 mg

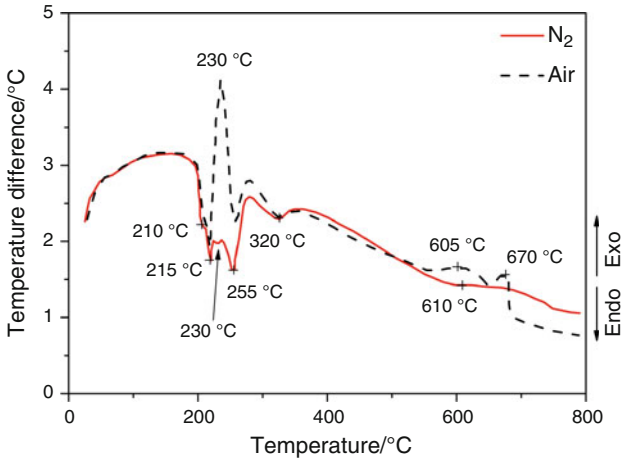

Fig. 4 DTA curves of **1** in nitrogen (*solid line*) and air (*dashed line*), as measured in situ in the online coupled TG/DTA-MS system. N_2 flow 130 mL/min, heating rate 10 °C/min, initial mass 8.71 mg; air flow 130 mL/min, heating rate 10 °C/min, initial mass 9.60 mg

Evolved gas analysis in nitrogen and in air atmospheres by online TG/DTA-EGA-MS and TG-EGA-FTIR systems

Figure 5 shows the evolution curves of gases as ion currents of characteristic mass fragments of the identified gaseous species versus temperature evolved from **1** in nitrogen and in air in comparison as recorded by online TG/DTA-EGA-MS. Figure 6 shows the evolution profiles of gases from **1** in air as recorded by online TG-EGA-FTIR.

According to EGA-MS in nitrogen, the first decomposition step (205–275 °C) started with the evolution of carbon disulfide (CS_2), ammonia (NH_3) and hydrogen chloride (HCl) with characteristic ion fragments of $m/z = 76$, $m/z = 17$ and $m/z = 36$, respectively (Fig. 5). Interestingly, sulfur dioxide ($m/z = 64$, SO_2), carbonyl sulfide ($m/z = 60$, COS) and carbon dioxide ($m/z = 44$, CO_2) were also evolved in nitrogen. In air, besides above-mentioned gaseous species, such as CS_2, NH_3, SO_2, COS and CO_2, the evolution of cyanamide ($m/z = 42$, H_2NCN) and hydrogen cyanide ($m/z = 27$, HCN) was recorded in the first decomposition step (205–275 °C) by EGA-MS (Fig. 5).

EGA-FTIR analysis in air confirmed the evolution of the same gases in the temperature interval of 205–275 °C as recorded by EGA-MS. However, the evolution of HNCS was detected in addition by EGA-FTIR (Fig. 6). The evolution of HCl was not detected by EGA-FTIR when using initial mass of **1** less than 10 mg. However, while using **1** with initial mass higher than 40 mg, the evolution of HCl was detected by EGA-FTIR in air. However, higher sample mass could not be used for the study because of an obstruction, a jam occurred in the FTIR-spectroscopic gas cell piping during thermal analysis at temperatures above 400 °C.

The evolution of NH_3 and HNCS was characteristic of the second decomposition step (275–425 °C) as detected by EGA-FTIR (Fig. 6). The evolution of NH_3 could not be unambiguously determined from EGA-MS study (Fig. 5) in neither of atmospheres. However, the evolution of COS and the ongoing evolution of SO_2 (Figs. 5, 6) was detected by both systems in both atmospheres.

Thereafter, in the third decomposition step in nitrogen (405-750 °C) and in air (405–700 °C), the release of CO_2, H_2NCN, SO_2 and HCl was detected by EGA-MS (Fig. 5). According to EGA-FTIR, the evolution of CO_2 and H_2NCN was very strong in this step. Although the vibrations in the region of 2220–2300 cm^{-1} (Fig. 6) could be characteristic of both H_2NCN and HNCO, the evolution of H_2NCN corresponds to that detected by EGA-MS. Also SO_2 and some HNCS released at temperatures above 400 °C, but no evolution of HCl was detected by EGA-FTIR in air.

Discussion of thermal analysis results

The sequence of gases evolved was more apparent and easier to follow by EGA-FTIR than by EGA-MS. Hence the sequence of the evolved gaseous species was presented in the order they appared by EGA-FTIR. Gaseous CS_2 and NH_3 released first in both atmospheres, indicating the decomposition of two neighboring thiourea ligands in the melt according to the reaction (1) [15–20]:

$$2SC(NH_2)_{2(l)} = CS_{2(g)} + 2NH_{3(g)} + H_2NCN_{(l,g)} \quad (1)$$

An absorption peak was detected at 2070 cm^{-1} in the FTIR spectrum of the solid residue of **1** heated up to 225 °C in air (See Fig. 5 in [6]). This peak could be assigned to the stretching vibration of both thiocyanate (SCN) and hydrogen bonded RNH_3^+ groups [12]. The presence of this peak

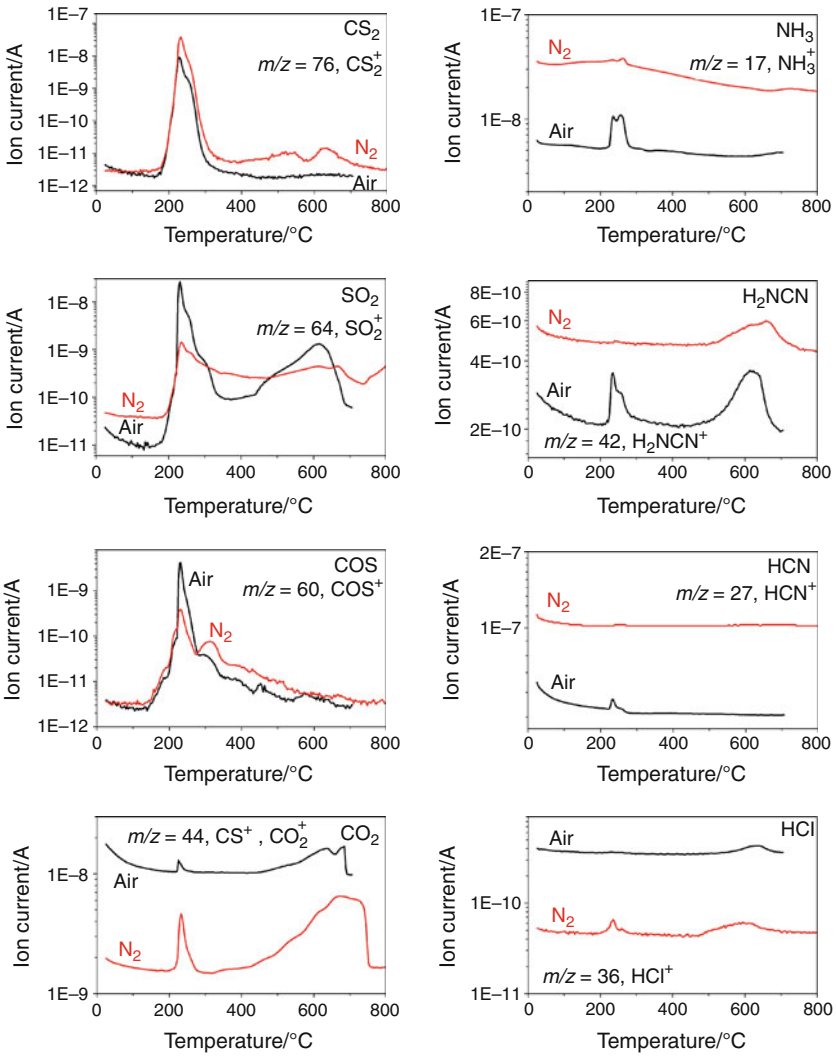

Fig. 5 Gas evolution profiles of various gaseous species, represented by their characteristic mass spectroscopic ion fragments, from **1** in nitrogen and in air, as measured by in situ online coupled TG/DTA-EGA-MS system. N_2 flow 130 mL/min, heating rate 10 °C/min, initial mass 8.71 mg; air flow 130 mL/min, heating rate 10 °C/min, initial mass 9.60 mg

indicates that probably part of $SC(NH_2)_2$ isomerised into ammonium thiocyanate (NH_4SCN), as it has also been observed during the thermal decomposition of different complex compounds with thiourea ligand such as $Cd(SCN_2H_4)_2Cl_2$, $Zn(SCN_2H_4)_2Cl_2$, $Cu(SCN_2H_4)_3Cl$ [12, 15, 21], and $SC(NH_2)_2$ [18]. The isomerisation of $SC(NH_2)_2$ could be presented as Eq. 2 [18]:

$$SC(NH_2)_{2(l)} + \text{Heat} = NH_4SCN_{(l)} \quad (2)$$

The decomposition of both $SC(NH_2)_2$ and NH_4SCN could be responsible for the evolution of HNCS and NH_3 as detected by EGA-FTIR in air. The release of HNCS and NH_3 could occur according to the reactions (3, 4), as reported previously [15, 20].

$$NH_4SCN_{(l)} = HNCS_{(g)} + NH_{3(g)} \quad (3)$$

$$SC(NH_2)_{2(l)} = HNCS_{(g)} + NH_{3(g)} \quad (4)$$

Closely after the evolution of CS_2, the release of SO_2 and COS started (Figs. 5, 6), implying to the oxidation of CS_2 vapor according to Eq. 5 [15–17, 19, 20]:

$$CS_{2(g)} + 1.5O_{2(g)} = SO_{2(g)} + COS_{(g)} \quad (5)$$

An exothermic effect with maximum at 230 °C in air (Fig. 4) could be explained by this oxidation process. In nitrogen, DTA curve of **1** (Fig. 4) showed only a weak endothermic effect at 230 °C. Probably, partial oxidation occurred simultaneously as the evolution of SO_2 and COS was detected also in inert atmosphere (Fig. 5). An additional TG/DTA/EGA-FTIR measurement of **1** was performed on SetSys-Evolution instrument connected to Nicolet 380 FTIR spectrometer in the Laboratory of Inorganic Materials at Tallinn University of Technology (Tallinn, Estonia). Evolution of SO_2 and COS in this decomposition step was confirmed by using pure argon atmosphere. Thus, the oxygen source, leading to the oxidation in an inert atmosphere could be originated from oxygen contamination in **1**, surroundings of the open measuring systems or certain level of oxygen impurities in the inert purge gas used. For example, Onishi et al. [22]

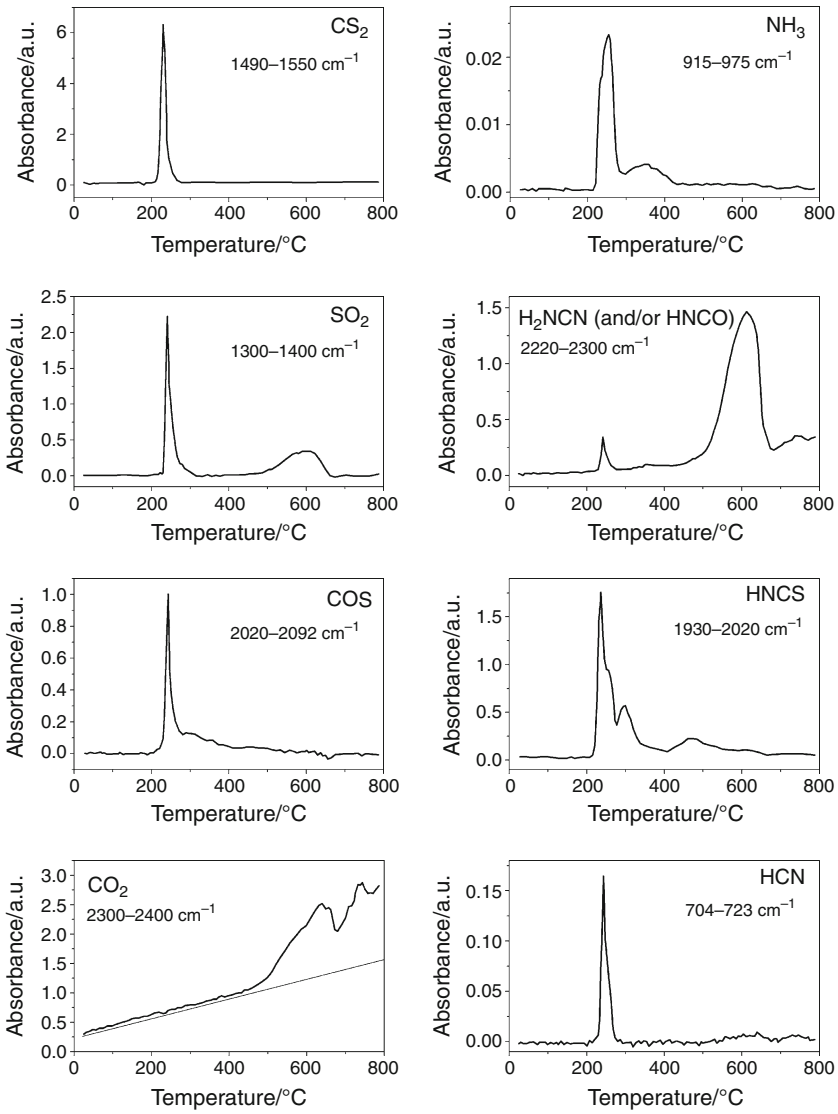

Fig. 6 Evolution profiles of gaseous species from **1** in air, as measured by in situ TG-EGA-FTIR system (air flow 130 mL/min, heating rate 10 °C/min, initial mass 8.69 mg)

pointed out, that although they used high purity argon for the thermal analysis, it still contained small amount of oxygen (<10 ppm), what was responsible for the oxidation process. Besides, small amount of oxygen (0.4 mass%) was detected in **1** by the energy dispersive spectroscopy (EDS) analysis performed on the Oxford Instruments INCA Energy system using the accelerating voltage of 7 kV in the Centre for Materials Research at Tallinn University of Technology (Tallinn, Estonia). Oxygen contamination could be originated from the preparation of **1** as $SC(NH_2)_2$ could be hydrolyzed into colloidal sulfur and urea ($OC(NH_2)_2$) in highly acidic aqueous solution.

In air, the evolution of HCN was detected at temperatures above 230 °C by both the EGA-MS and EGA-FTIR (Figs. 5, 6). Formation of HCN can be considered as the oxidation product of HNCS according to the reaction (6) [15, 19, 20]:

$$HNCS_{(g)} + O_{2(g)} = HCN_{(g)} + SO_{2(g)} \quad (6)$$

In addition to the reaction (1), the evolution of H_2NCN at 240 °C in air might originate from the metal sulfide formation proposed by Krunks et al. [15]. The formation of In_2S_3 in the first decomposition step upon thermal decomposition of **1** in air has been confirmed by XRD [6]. Thus, the reaction characterizing the formation of In_2S_3 and the evolution of H_2NCN together HCl could be supposed as follows (7):

$$2InCl_3 + 3SC(NH_2)_{2(l)} = In_2S_{3(s)} + 3H_2NCN_{(l,g)} + 6HCl_{(g)} \quad (7)$$

H_2NCN vapors could condensate on the windows and mirrors of the IR gas cell, as it has been observed during the evolved gas analysis of the $Zn(SCN_2H_4)_2Cl_2$ [16], polymerization of H_2NCN could be also possible [23].

The second decomposition step (275–405 °C) was an endothermic process with a DTA maximum at 320 °C (Fig. 4) and showed closely similar mass losses in both atmospheres (Fig. 3). Evolution of HNCS and NH_3 was characteristic of this decomposition step. Reappearance of HNCS and NH_3 at temperatures higher than characteristic of their primary formation has also been observed during the thermal decomposition of $SC(NH_2)_2$ in helium and air atmospheres [17]. Probably an intermediate is formed in the first decomposition step, which at higher temperatures decomposes with release of HNCS and NH_3, as also speculated in [18]. According to EGA-FTIR study (Fig. 6), the evolution of HNCS continues even in the third decomposition step, at temperatures above 400 °C. It could be expected that HNCS oxidizes into HCN, but evolution of HCN was not detected in the second and third decomposition steps by either of the measuring methods, indicating that probably its concentration was very low.

Evolution of the gaseous species such as SO_2, CO_2, H_2NCN, and HCl was characteristic of the third decomposition step in nitrogen (405–750 °C) and in air (405–700 °C) according to EGA-MS (Fig. 5). EGA-FTIR confirms the evolution of SO_2, H_2NCN, and CO_2.

The release of SO_2 around 600 °C in both atmospheres, nevertheless very weak in nitrogen, could be due to the oxidation of In_2S_3 (8):

$$In_2S_{3(s)} + 4.5O_{2(g)} = In_2O_{3(s)} + 3SO_{2(g)} \quad (8)$$

According to EGA-MS, the evolution profile of H_2NCN was similar to that of HCl in both atmospheres (Fig. 5) indicating that both gases probably originated from the same or concurrent reactions. The evolution of H_2NCN could be due to the degradation of a polymerized phase originated from H_2NCN or due to the decomposition of indium cyanamide ($In_{2.24}(NCN)_3$), an intermediate solid product of **1** in the third decomposition step as was confirmed by XRD in our previous study [6].

It could be supposed that part of $InCl_3$ which did not react to form In_2S_3 according to the reaction (7) reacted with H_2NCN formed in the first decomposition step at temperatures below 300 °C or when a polymerized phase decomposes:

$$InCl_3 + H_2NCN \rightarrow In_{2.24}(NCN)_3 + HCl \uparrow \quad (9)$$

The observation that evolution of H_2NCN was much stronger in the third decomposition step compared to that in the first step refers that H_2NCN was captured into a condensed phase at temperatures characteristic of the second decomposition step.

TG analysis showed that the mass loss in the third decomposition step was higher in nitrogen compared to that in air (Fig. 3), and the total mass loss was higher than expected independent of the atmosphere indicating disappearance of species containing indium from the sample. Likely, $InCl_3$ with its total vapor pressure of ca 100 kPa at temperatures around 500 °C [14] was responsible for this effect. In the vapor phase indium chloride could be present in the form of $InCl_3$ or its dimer, In_2Cl_6 [24]. Thus, higher mass loss in nitrogen was obviously due to the vaporization of indium chloride, while in air it easily oxidizes forming In_2O_3, which remains in the condensed phase. The mass loss due to volatilization of In_2S_3 in nitrogen was not notable as vapor pressure of In_2S_3 at temperatures close to 800 °C is ca. 1 Pa [25].

The evolution of CO_2 from 450 °C up to the end of thermal degradation in both atmospheres (Figs 5, 6) was probably due to the combustion of solid residues containing carbon present in the matter. The oxidative atmosphere with additional heat effect from exothermic process above 550 °C promote degradation reactions resulting the end of decomposition process already at 700 °C in air, while in nitrogen it lasted up to 750 °C.

Conclusions

It has been shown that the $InCl_3$ and $SC(NH_2)_2$ in the molar ratio of 1:3 in an aqueous solution interact to form complex compound *mer*-trichlorotris(thiourea)-indium(III) ($In(tu)_3Cl_3$, **1**), a precursor for In_2S_3 films in the CSP process. Single crystal X-ray diffraction structural analysis improved the formerly reported structural model as the disordered asymmetric complex molecules situated on an inversion centre has now been successfully separated and described. The indium cation is octahedrally coordinated by the three thiourea molecules and three chloride anions forming meridional isomers in all three crystallographic forms present in the conventional unit cell.

Thermal decomposition of **1** contained three mass loss steps in the temperature range of 205–750 °C in nitrogen and 205–700 °C in air atmospheres. The final decomposition product of **1** in air was In_2O_3, the final product in nitrogen comprised In_2S_3 and In_2O_3. The total mass loss of **1** was higher than expected in both atmospheres (but especially in inert atmosphere) indicating release of some volatile indium species, probably of $InCl_3$ known with its high vapor pressure, mainly in dimeric In_2Cl_6 form [26], which could not be detected within the range of $m/z = 1$–300 of the quadrupole mass spectrometer [27]. The extent of non-reacted species containing $InCl_3$ can be reduced by application of a high excess of thiourea in spray solution [6], what may shift the processes towards indium sulfide formation and helps to avoid loss of indium.

The main decomposition processes of **1** in inert and air atmospheres occurred in the temperature region of 205–275 °C. The gaseous products released in nitrogen

were CS_2, NH_3, and HCl according to EGA-MS. Evolution of SO_2, COS, and CO_2 were also detected in both atmospheres, although during the thermal decomposition of **1** in nitrogen only endothermic effects were observed. In air, besides to all above named gaseous products, the evolution of H_2NCN and HCN were detected in the first decomposition step (205–275 °C) by both EGA-MS and EGA-FTIR. It should be noted, that the evolution of HNCS in the temperature interval of 205–670 °C in air was detected only by EGA-FTIR. The second evolution of CO_2, H_2NCN, SO_2 and HCl were detected above 450 °C in both atmospheres by both measuring methods.

Chemical reactions occurring during the thermal decomposition of **1** were presented including the formation reaction of In_2S_3 in the first decomposition step, at temperatures below 300 °C.

Results on the formation and the molecular structure of *mer*-trichlorotris(thiourea)-indium(III) (**1**) and its thermal behavior in inert and oxidative atmospheres provided important data to determine the solution composition and thermal conditions in oder to deposit In_2S_3 thin films with device quality properties by CSP.

Acknowledgements Funding by the Estonian Ministry of Education and Research (Target Financing Project SF0140092s08) and Estonian Science Foundation grants ETF6954 and ETF7788 are gratefully acknowledged. The authors also thank Dr. V. Mikli for EDS analysis and Dr. K. Tõnsuaadu for TG/DTA/EGA-FTIR measurements on SetSys-Evolution instrument connected to Nicolet 380 FTIR spectrometric gas cell. A diffractometer purchase grant from the Hungarian National Office for Research and Technology (MU-00338/2003) is gratefully acknowledged.

References

1. Krunks M, Kärber E, Katerski A, Otto K, Oja Acik I, Dedova T, Mere A. Extremely thin absorber layer solar cells on zinc oxide nanorods by chemical spray. Sol Energy Mater Sol Cells. 2010; 94:1191–5.
2. Buecheler S, Corica D, Guettler D, Chirila A, Verma R, Müller U, Niesen TP, Palm J, Tiwari AN. Ultrasonically sprayed indium sulfide buffer layers for Cu(In, Ga)(S, Se)$_2$ thin-film solar cells. Thin Solid Films. 2009;517:2312–5.
3. Kim W-T, Kim C-D. Optical energy gaps of β-In_2S_3 thin films grown by spray pyrolysis. J Appl Phys. 1986;60:2631–3.
4. John TT, Bini S, Kashiwaba Y, Abe T, Yasuhiro Y, Sudha Kartha C, Vijayakumar KP. Characterization of spray pyrolysed indium sulfide thin films. Semicond Sci Technol. 2003;18:491–500.
5. Otto K, Katerski A, Mere A, Volobujeva O, Krunks M. Spray pyrolysis deposition of indium sulfide thin films. Thin Solid Films. 2011;519:3055–60.
6. Otto K, Oja Acik I, Tõnsuaadu K, Mere A, Krunks M. Thermoanalytical study of precursors for In_2S_3 thin films deposited by spray pyrolysis. J Therm Anal Calorim. 2011. doi:10.1007/s10973-011-1507-8.
7. Malyarik MA, Ilyukhina AB, Petrosyants SD, Buslaev YuA. Geometric isomers in indium(III) halo complexes: preparation and crystal structure of trichlorotris(thiourea)indium. Zh Neorg Khim Russ (Russ J Inorg Chem). 1992;37:1504–8.
8. Sheldrick GM. A short history of SHELX. Acta Crystallogr. 2008;A64:112–22.
9. NIST Chemistry WebBook Standard Reference Database No 69, June 2005 Release. http://webbook.nist.gov/chemistry.
10. Spek AL. Structure validation in chemical crystallography. Acta Crystallogr. 2009;D65:148–55.
11. International Centre for Diffraction Data (ICDD). Powder Diffraction File (PDF). PDF-2 Release 2009.
12. Krunks M, Madarász J, Leskelä T, Mere A, Niinistö L, Pokol G. Study of zinc thiocarbamide chloride, a single-source precursor for zinc sulfide thin films by spray pyrolysis. J Therm Anal Calorim. 2003;72:497–506.
13. Madarász J, Bombicz P, Okuya M, Kaneko S. Thermal decomposition of thiourea complexes of Cu(I), Zn(II), and Sn(II) chlorides as precursors for the spray pyrolysis deposition of sulfide thin films. Solid State Ion. 2001;141–142:439–46.
14. Brunetti B, Piacente V, Scardala P. A torsion study on the sublimation process of $InCl_3$. J Chem Eng Data. 1998;43:101–4.
15. Krunks M, Madarász J, Hiltunen L, Mannonen R, Mellikov E, Niinistö L. Structure and thermal behaviour of dichlorobis(thiourea)cadmium(II), a single-source precursor for CdS thin films. Acta Chem Scand. 1997;51:294–301.
16. Madarász J, Krunks M, Niinistö L, Pokol G. Evolved gas analysis of dichlorobis(thiourea)zinc(II) by coupled TG-FTIR and TG/DTA-MS techniques. J Therm Anal Calorim. 2004;78:679–86.
17. Madarász J, Pokol G. Comparative evolved gas analysis on thermal degradation of thiourea by coupled TG-FTIR and TG/DTA-MS instruments. J Therm Anal Calorim. 2007;88:329–36.
18. Wang S, Gao Q, Wang J. Thermodynamic analysis of decomposition of thiourea and thiourea oxides. J Phys Chem B. 2005; 109:17281–9.
19. Madarász J, Bombicz P, Okuya M, Kaneko S, Pokol G. Comparative online coupled TG-FTIR and TG/DTA-MS analyses of the evolved gases from thiourea complexes of $SnCl_2$ tetrachloropenta(thiourea) ditin(II), a compound rich in thiourea. J Anal Appl Pyrolysis. 2004;72:209–14.
20. Krunks M, Leskelä T, Mannonen R, Niinistö L. Thermal decomposition of copper(I) thiocarbamide chloride hemihydrate. J Therm Anal Calorim. 1998;53:355–64.
21. Krunks M, Leskelä T, Mutikainen I, Niinistö L. A thermoanalytical study of copper(I) thiocarbamide compounds. J Therm Anal Calorim. 1999;56:479–84.
22. Onishi A, Thomas PS, Stuart BH, Guerbois JP, Forbes SL. TG-MS analysis of the thermal decomposition of pig bone for forensic applications. J Therm Anal Calorim. 2008;1:87–90.
23. Porter AEA, Sammes PG. Comprehensive organic chemistry, vol. 4. Oxford: Pergamon Press; 1979.
24. Defoort F, Chatillon C, Bernard C. Mass-spectrometric study of (indium + chlorine)(g) enthalpies of formation of InCl(g), In_2Cl_2(g), In_2Cl_4(g), $InCl_3$(g), and In_2Cl_6 (g). J Chem Thermodyn. 1988;20:1443–56.
25. Ferro D, Piacente V, Scardala P. Sublimation behavior of indium trisulfide studied by a simultaneous torsion and Knudsen technique. J Mater Sci Lett. 1988;7:1301–4.
26. Fadeev VN, Fedorov PI. Vapor pressure in the In-$InCl_3$ system. Zh Neorg Khim. 1964;9:378–80.
27. Sawada Y, Aoyama T, Seki S, Arii T, Senda T, Ozao R. Thermal analyses of transparent conducting films, part 2: oxide formation from indium chloride. In: Proceedings of the NATAS annual conference on thermal analysis and applications, Albuquerque, NM, vol 3, Sept 22–24, 2003, pp 158/1–158/6.